Control and Optimization in Applied Mathematics (COAM)
Vol. 2, No. 2, Autumn-Winter 2017(61-76), ©2016 Payame Noor University, Iran

Optimal Shape Design for a Cooling Pin Fin Connection Profile

S. H. Hashemi Mehne*[1], K. Javadi[2],

[1]Department of Avionics, Aerospace Research Institute,
P.O. Box. 14665-834, Tehran, Iran,
[2]Department of Aerospace Engineering, Sharif University of Technology
P.O. Box. 11365-11155 , Tehran, Iran

Received: Nov 17, 2017; **Accepted:** Apr 29, 2019.

Abstract. A shape optimization problem of cooling fins for computer parts and integrated circuits is modeled and solved in this paper. The main purpose is to determine the shape of a two-dimensional pin fin, which leads to the maximum amount of removed heat. To do this, the shape optimization problem is defined as maximizing the norm of the Nusselt number distribution at the boundary of the pin fin's connection profile. The governing differential equations are solved in solid and fluid phases separately. In order to formulate the optimization problem with finite dimensions, the shapes of the profiles are parameterized with cubic polynomials. Due to the lack of an explicit relation between the objective function and the geometric parameters, an approximate modeling method is used for the optimization process. The proposed method starts with three initial points. Then, the governing differential equations are solved for each of the profiles related to the initial points. The new step in this iterative process involves calculations based on a polynomial interpolation within the resulting Nusselt number norms. A numerical example is given to show the implementation and accuracy of the method..

Keywords. Approximation, Heat transfer, Optimization, Shape optimization.

MSC. 49Q10; 49M37.

∗ Corresponding author
hmehne@ari.ac.ir, kjavadi@sharif.edu
http://mathco.journals.pnu.ac.ir

1 Introduction

The problem of heat reduction and the cooling of surfaces subjected to heat sources is a significant problem in high technology. There is industrial interest in miniaturization arising from savings in volume, cost, weight and materials. Such a miniaturization requirement alongside performance improvement raises complex heat-exchange questions.

In computer manufacturing, for example, heat removal from integrated circuits is essential, and developing more efficient and smaller microprocessors requires new heat challenges to be resolved.

The pin fin heat sink is a well-known tool to increase heat removal in computer mainboards. It is also used in other applications where metallic surfaces are responsible for heat transfer. The use of an appropriate pin fin heat sink leads to increased performance and reliability of electronic devices. Due to cost and volumetric constraints, the problem of designing the pin fin heat sink is important. The length, geometrical shape, and cross section of single pin fins, along with their number and arrangement in the heat sink plate, are the effective parameters in current designs. Hamadneh et al. [1] demonstrated the use of particle swarm optimization to find the optimum dimensions of a pin fin for the minimally generated entropy. Moreover, the effect of the fin's cross section and the arrangement of an array of fins in the corresponding plate were analyzed in this work. The minimum generated entropy combines the effects of heat resistance and pressure changes in a heat sink. The results of [1] indicated that the preferred fin profile is very dependent on the geometric parameters.

In the work of [2], topology optimization of an air-cooled heat sink was presented by considering heat conduction and side-surface convection. The heat transfer and flow performance of the optimum sink were also evaluated experimentally. Next, heat sink dimension optimization was reported by [3], who minimized the heat sink's temperature with a prescribed pressure drop and given heat production. In the study by [4], an analytical solution for an unsteady temperature distribution in multi-layer composite fins was given. The effect of the cooling rate was also studied for the case of a fixed fin diameter. The problem of optimizing a heat sink with an array of cylindrical pin fins was studied by [5]. The entropy generation rate was minimized in terms of the overall performance of the heat sink by considering the pin diameter, approach velocity, and heat sink thermal conductivity as the design parameters. The problem has also been modeled as a constrained mathematical programming. In an experimental approach to obtain the optimal pin fin height, the base size and cross-sectional area were investigated by [6]. The thermal resistances were treated as proxies for the heat sink thermal performance, which was maximized. Minimum weights, ease of manufacturing and better thermal performance are the results of this study.

A special pin fin heat sink for cooling Li-ion batteries was studied to determine the optimum pin height and arrangement by [7]. Their work was based on a three-dimensional transient thermal analysis on some predefined cases, and the authors compared their performance results with literature examples. In the study by [8], phase change material (PCM) based pin fin heat sinks were investigated to determine their optimum geometrical configuration. The considered design parameters were the number of fins, fin height, fin thickness and the base thickness. The

goal of optimization in this work was to maximize the operational time of the heat sink, where the Taguchi optimization method coupled with numerical solutions was used.

A multidisciplinary optimization was adopted by [9] to optimize a radial pin fin heat sink. The heat sink's thermal resistance and mass were minimized in this work based on the number of fin arrays, fin length and the space between fins as the design parameters. The results of [9] showed a 10–12% increase in the heat sink performance for the optimum designs.

In the work of [10], the temperature distribution and the parameters that affected the rate of heat transfer in a porous pin fin were studied.

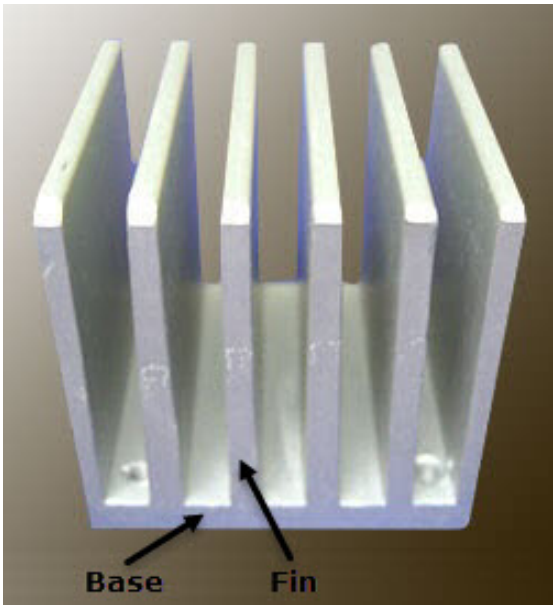

Figure 1: A typical heat sink with six pin fins and right-angle connections between the base and fins.

As denoted in Figure 1, a typical heat sink for electronic devices consists of some pin fins attached to a base. In this current investigation, our objective is to design a curve that connects a pin fin to its base in such a way that the heat removed from the bottom is maximized. As a first step, the effect of this profile on fin performance and the amount of heat removal is studied. Then, the Nusselt number distribution of the profile curve is introduced as a performance-measuring index. The curve is then parameterized with third-degree polynomials to model the problem as a finite dimensional optimization. Finally, approximate modeling is applied to the problem, and its performance is evaluated with a test case.

2 Primary Simulations

The aim of this work is to study the effect of the shape of the curve that connects the fin to its base, and to attempt to find the optimum shape. The problem is studied for a two-dimensional (2D) case.

As a first step, we consider a flat plate, which is exposed to a hot source at the bottom and convects heat to the other side. In this case, the heat transfer is solved using simple fin relations with a convective boundary condition, instead of solving the full governing equations for a fluid. A FORTRAN program was developed that solves the heat convection equations of the fin and plate with the finite element method. The geometry and boundary conditions for two cases (i.e. right angle and circular) are shown in Figure 2.

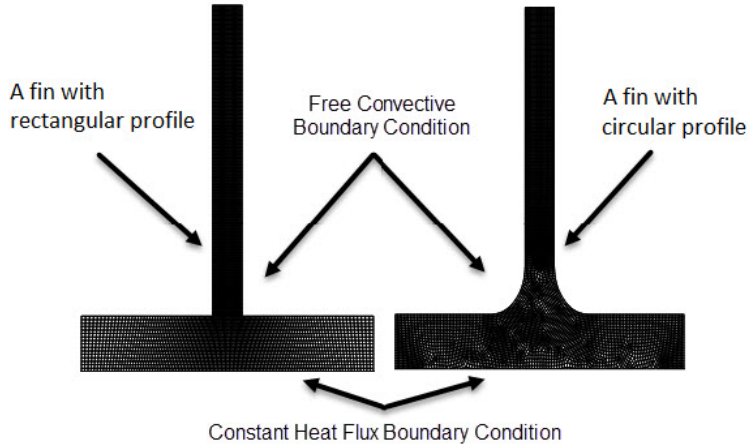

Figure 2: Two different pin fin connection profiles, their bases and the boundary conditions.

The results show that, in this case, a greater convective surface area will result in better fin performance, because the fluid dynamics of the fin are not considered. Therefore, the right-angle profile, which has the greater surface area, is the best profile in this simple case. This shows that the profile shape affects the thermal performance of the fin. In the next sections, more complicated and accurate model regarding heat and flow is considered.

3 Problem Statement

Let us consider a symmetric 2D pin fin that is influenced by a fixed hot temperature from the bottom plate and cooled by air blowing from impinging jets. The flow speed is in the real range for CPU cooling, equal to 1 m/s.

The fin's geometry, coordinate system and domain are shown in Figure 3. The objective of the present optimal shape design is to find the curve connecting points, (c, a) and (d, b), in such a way that the cooling performance of the fin is maximized. A quantity that can be used for optimization is the Nusselt number on the fin's surface. The Nusselt number is a dimensionless heat-transfer coefficient that is defined as the ratio of the convective heat transfer to the conductive fluid heat transfer [12]. This quantity is a criterion of flow development and the heat transfer rate at the surface. Therefore, the shape that has the maximum Nusselt number has the best heat transfer rate and consequently the best heat removal property.

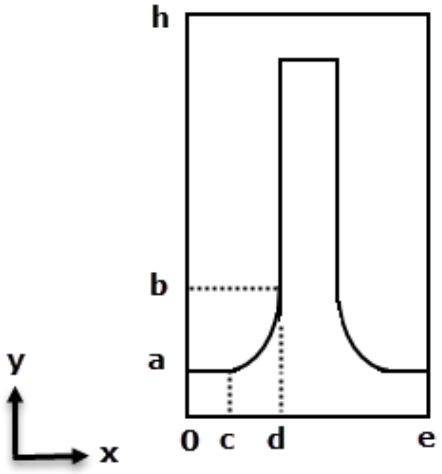

Figure 3: Geometry of a pin fin connection and its base.

Therefore, the problem is to find the curve connecting points (c, a) and (d, b) represented by $y = f(x)$ such that the related Nusselt numbers on this curve can be maximized. Let $N(f, x)$ denote the value of the Nusselt number at a point on the curve with x coordinate; then, a natural way to construct the performance index is to use the L_1-norm as follows. Using this method, all contributions of Nusselt numbers are added:

$$I(f) = \int_c^d |N(f, x)|dx \tag{1}$$

Let us define the set of admissible profiles as:

$$U_{ad} = \{f(.) \in C^1([c, d]) \mid f(c) = a, f(d) = b\} \tag{2}$$

where $C^1([c, d])$ shows the set of all continuously differentiable functions on $[c, d]$. Then, the optimal shape design problem can be expressed as:

$$\text{Maximize} \quad I(f) \tag{3}$$

Subject to:

$$f \in U_{ad} \tag{4}$$

In order to find $N(f, x)$, we have to solve the governing equations of fluid dynamics and solid interactions, which will be given in the next section.

4 Governing Equations

In the second viewpoint, the equations of convective heat transfer within the fin, mass conservation equations, momentum equation, and fluid energy for the fluid around the fin are solved simultaneously. This is a well-known approach to solving coupled solid and fluid equations [11].

Developing a computer code that solves the coupled heat transfer equations within a fluid and solid is an intricate task, especially for complex geometries. Therefore, here, a commercial computational fluid dynamics (CFD) software is utilized.

Figure 4 shows the problem geometry and boundary conditions. It is assumed that the airflow blows to the fin from the top and exits from the sides, after meeting the fin and moving across it.

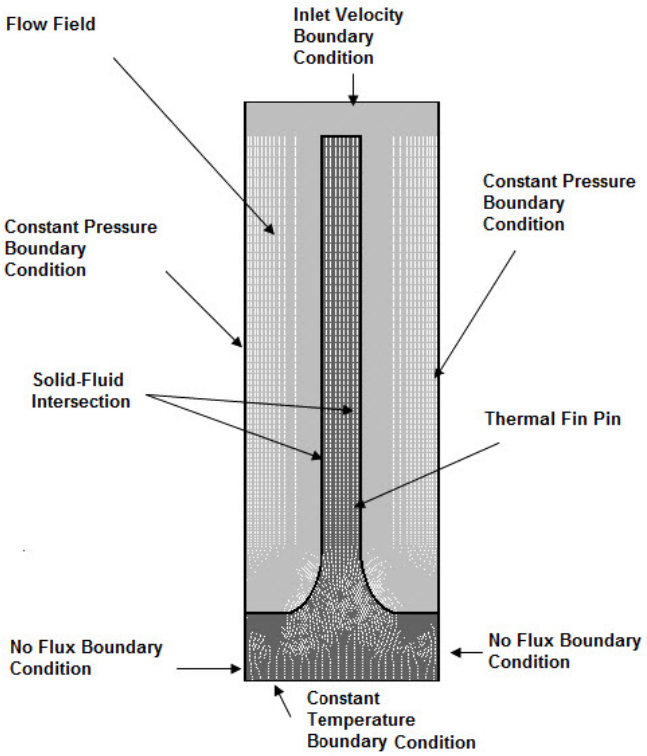

Figure 4: Problem geometry with boundary conditions and grid.

As this problem is faced with solid and fluid phases, the governing equations should be solved independently and simultaneously. Due to synchronization and coupling, there is no need to implement any particular boundary condition at the intersections because it is resolved automatically.

For the solid part, the transfer equation is the mass conservation equation, which is simplified in the present case and is reduced to conductive heat transfer expressed by the Fourier relation.

In the fluid phase, we must consider the mass conservation, momentum and energy equations. As the flow is turbulent, the $(k-\epsilon)$ turbulent model is used. Therefore, assuming an incompressible, steady, 2D, turbulent flow with Reynolds averaging, the governing equations in the fluid phase are as follows:

Mass conservation equation:

$$\frac{\partial \overline{U_i}}{\partial x_i} = 0 \tag{5}$$

Momentum conservation equation:

$$\frac{\partial}{\partial x_j}(-\rho\overline{u_i u_j})\rho\overline{U_j}\frac{\overline{U_i}}{\partial x_j} = -\frac{\partial p}{\partial x_i} + \frac{\partial}{\partial x_j}\left[\mu\left(\frac{\partial\overline{U_i}}{\partial x_j} + \frac{\partial\overline{U_j}}{\partial x_i}\right)\right] \tag{6}$$

Energy conservation equation:

$$\rho\frac{\partial}{\partial x_j}(\overline{U_j T}) = \frac{\partial}{\partial x_j}\left[\left(\frac{\mu_l}{\mathrm{Pr}_l} + \frac{\mu_t}{\mathrm{Pr}_t}\right)\frac{\partial\overline{T}}{\partial x_j}\right] \tag{7}$$

Turbulent kinetic energy conservation and its vanishing rate:

$$\frac{D\rho k}{Dt} = \tau_{ij}\frac{\partial\overline{U_i}}{\partial x_j} - \beta^*\rho\omega k + \frac{\partial}{\partial x_j}\left[(\mu + \sigma_k\mu_t)\frac{\partial k}{\partial x_j}\right] \tag{8}$$

$$\frac{D\rho\omega}{Dt} = \frac{\gamma}{\nu_t}\tau_{ij}\frac{\partial\overline{U_j}}{\partial x_j} - \beta\rho\omega^2 + \frac{\partial}{\partial x_j}\left[(\mu + \sigma_\omega\mu_t)\frac{\partial\omega}{\partial x_j}\right] + 2\rho(1-F_1)\sigma_{\omega^2}\frac{1}{\omega}\frac{\partial k}{\partial x_j}\frac{\partial\omega}{\partial x_j} \tag{9}$$

In these equations, $\frac{D}{Dt} = \frac{\partial}{\partial t} + u_i\frac{\partial}{\partial x_i}$ is the Lagrangian derivative, F_1 is the switch function in the $(k-\epsilon)$ model, k is the turbulent kinetic energy, Pr is the Prandtl number, Re is the Reynolds number, $\overline{T}$ is the average temperature, U_i are the instantaneous velocity components, $\overline{U_i}$ are the mean velocity components, u_i are the fluctuation velocity components, $\overline{u_i u_j}$ are the Reynolds stresses, β, β^* and γ are empirical constants in the shear stress transport (SST) model, μ is the viscosity, μ_t is the Eddy kinematic viscosity, ρ is the density, σ, σ_ω and σ_{ω^2} are the empirical constants in the SST model, τ_{ij} denotes the Reynolds stress tensor, and ω stands for the specific dissipation rate. For more information about the constants of the equations above, see [11].

4.1 Boundary Conditions

As depicted in Figure 4, there are two boundary conditions in the solid part:

1- At the bottom surface, which is subjected to a fixed temperature, a constant temperature boundary condition is imposed, that is:

$$T|_{y=0} = 350^\circ K \tag{10}$$

2- On the side boundaries, which assumes that there are other fins and that heat cannot pass through them. Therefore, no flux boundary conditions are considered as follows, where $n = -\vec{i}$ is the external normal vector:

$$\frac{\partial T}{\partial n}|_{x=0,y\le a} = \frac{\partial T}{\partial n}|_{x=e,y\le a} = 0 \tag{11}$$

On the other hand, there are two types of boundary conditions in the fluid phase:

1- The assumption that in the inlet section a flow of 1 ms^1 blows on the fin from above requires an inlet velocity boundary condition. The condition is:

$$U_1|_{y=h} = 0,\ U_2|_{y=h} = -1\frac{m}{s} \tag{12}$$

2- On the boundaries, it is assumed that the blowing flow enters the atmosphere after passing through the fin. This requires constant pressure boundary conditions as follows:

$$p|_{x=0,x=e} = P_\infty \tag{13}$$

5 Initial Numerical Simulation

First, the mesh of the solution domain was generated. As can be seen in Figure 4, a non-uniform mesh with clustering near the walls was constructed to predict the near wall points perfectly. The governing equations were transformed to a set of algebraic equations using finite volume methods. Conservation of momentum and mass were coupled together with the SIMPLE algorithm [16] and solved independently.

After solving for momentum and mass conservation, the energy and turbulence equations were solved. This procedure iterated until it reached convergence.

The solution was obtained for three profiles. Figures 5–7 show the results of the streamlines and temperatures obtained, respectively, for right angle, circular, and triangular profiles.

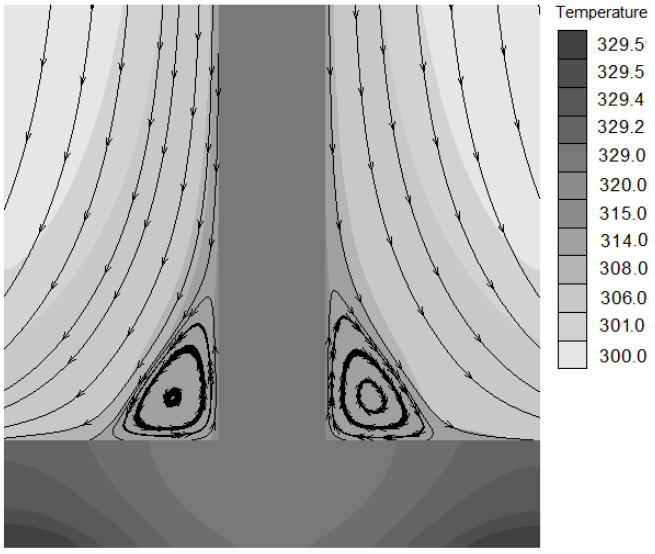

Figure 5: Streamlines and temperature contours for the rectangular profile.

As can be seen from these figures, the size and length of the vortex, which formed at the connecting point of the fin to its base, affected the convection rate and amount of removed heat from this region and transferred downstream.

These vortices did not have any considerable effect on the upstream regions. However, growths of the boundary layer on the fin's surface will have notable effects on the heat transfer rate. Therefore, managing the fin length and connection profile could affect the performance

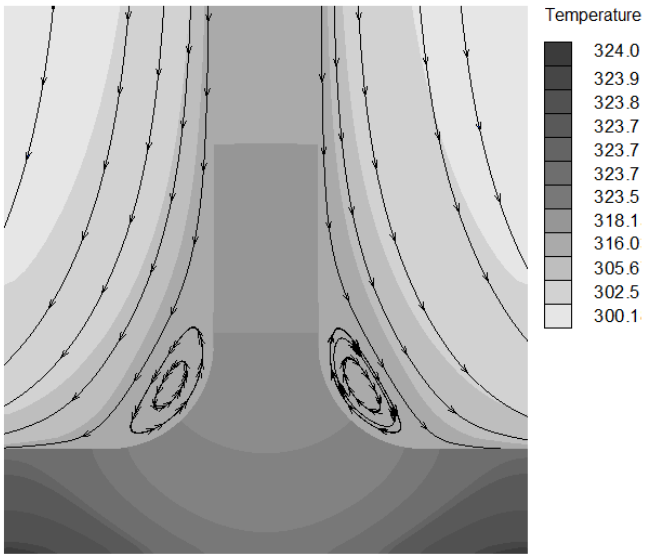

Figure 6: Streamlines and temperature contours for the circular profile.

of the fin. The optimum performance will cause a reduction in fan power, consequently saving electrical energy.

6 Shape Parameterization

To derive a method for solving this shape optimization problem, the set of admissible functions has to be parameterized. Here we assumed that every admissible curve constitutes two, third-degree polynomials as shown in Figure 8. The general form of these polynomials are as follows:

$$\text{Curve } C_1 : y = Ax^3 + Bx^2 + Cx + D \tag{14}$$

$$\text{Curve } C_2 : x = A'y^3 + B'y^2 + C'y + D' \tag{15}$$

Therefore, the problem of searching within the admissible curves is converted to the problem of searching within eight unknown coefficients: A, B, C, D, A', B', C', and D'. Some natural conditions will decrease the number of unknowns. This may be performed by defining a new variable α , as the x-location of the curve intersection and 45°. First, the conditions of connecting the curve to (c, a), (d, b) and $(d-\alpha, a+\alpha)$ should be imposed, which result in the following equations:

$$C_1 : \begin{cases} Ac^3 + Bc^2 + Cc + D = a \\ A(d-\alpha)^3 + B(d-\alpha)^2 + C(d-\alpha) + D = a + \alpha \end{cases} \tag{16}$$

$$C_2 : \begin{cases} A'(a+\alpha)^3 + B'(a+\alpha)^2 + C'(a+\alpha) + D' = d - \alpha \\ A'b^3 + B'b^2 + C'b + D' = d \end{cases} \tag{17}$$

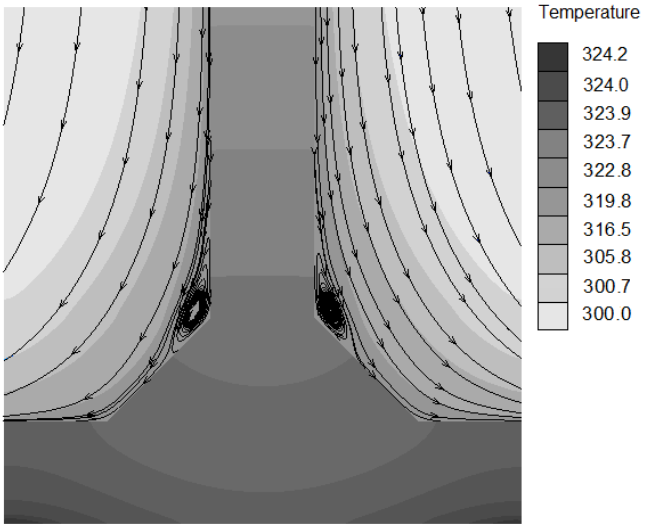

Figure 7: Streamlines and temperature contours for the triangular profile.

Moreover, there are tangential conditions. The curve C_1 should be tangential to the x-axis at $x = c$ and the curve C_2 should be tangential to the y-axis at $y = b$. Moreover, the two curves should meet each other with the same angle. If these tangential conditions are applied to the curves, the following equations arise:

$$C_1 =: \begin{cases} 3Ac^2 + 2Bc + C = 0 \\ 3A(d-\alpha)^2 + 2B(d-\alpha) + C = 1 \end{cases} \tag{18}$$

$$C_2 : \begin{cases} 3A'b^2 + 2B'b + C' = 0 \\ 3A'(a+\alpha)^2 + 2B'(a+\alpha) + C' = 1 \end{cases} \tag{19}$$

With this parameterization, every admissible shape corresponds to a unique value of α and vice versa. Therefore, it is sufficient to search for the optimum value of α that maximizes I, instead of searching for an optimum curve directly.

Assuming that the admissible curves should not exceed right-angle and triangular shapes, α is bounded as:

$$0 \leq \alpha \leq \frac{1}{2}(d-c) \tag{20}$$

We assume that $\alpha = 0$ corresponds to the right-angle case. Figure 8 shows some admissible shape samples corresponding to some values of α in this interval. In this example, the following constant geometric values are used:

$$a = 1, b = 3, c = 1, d = 2, e = 5, h = 8$$

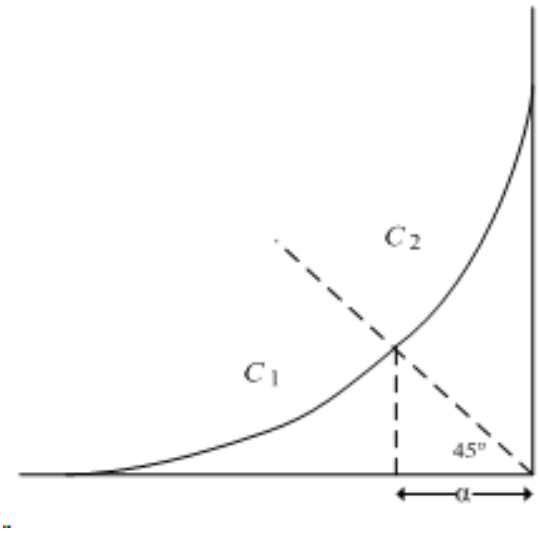

Figure 8: Curve parameterization of the connection profile.

7 Optimization Algorithm

Optimization methods are usually iterative processes, and when they are combined with CFD solvers, CFD solving is necessary at every iteration of the optimization algorithm. Due to the time-consuming nature of solving Eqs. (5–13), we utilized optimization methods that required only a low number of iterations. To this end, approximated modeling was used in the form of a surrogate optimization algorithm [13]. This method is usually applied to problems where the objective function is too complex or it does not have an explicit form. Convergence analyses and estimated error bounds to the solutions of these type of derivative-free methods have been studied in the literature, e.g. [14] and [15].

To start the method, an initial solution is required. Then, for each profile, the governing Eqs. (5–13) are solved via the CFD software independently. Then, the corresponding Nusselt number distribution is calculated and the related performance index (Eq. 2) is obtained for these three initial profiles. Therefore, there exist three points: namely $(\alpha_1, I(\alpha_1))$, $(\alpha_2, I(\alpha_2))$ and $(\alpha_3, I(\alpha_3))$. Then, a unique second-degree polynomial passes through all three points. This polynomial is used to approximately indicate the behavior of the performance index. The maximum of this polynomial is obtained by simple calculations, i.e. $(\alpha_{max}, I(\alpha_{max}))$. The worst point (i.e. that with the minimum performance index) within the initial three points is then replaced by $(\alpha_{max}, I(\alpha_{max}))$, and the method iterates until convergence occurs. The method is summarized as the following algorithm:

Start: Let $i = 1$ and choose three initial points: α_1, α_2 , and α_3. Choose $\epsilon > 0$ as the convergence checking parameter.

Step 1: Solve Eqs. (5–13) for the geometries related to α_1, α_2, and α_3.

Step 2: Calculate $I(\alpha_1)$, $I(\alpha_2)$, and $I(\alpha_3)$.

Step 3: Let $\alpha_{min} = \arg\min\{I(\alpha_i) \mid i = 1, 2, 3\}$.

Step 4: Find $P_2^i(\alpha)$, the second-degree polynomial passing through $(\alpha_1, I(\alpha_1))$, $(\alpha_2, I(\alpha_2))$ and $(\alpha_3, I(\alpha_3))$.
Step 5: Calculate the maximum of $P_2^i(\alpha)$ as $(\alpha_{max}, I(\alpha_{max}))$.
Step 6: If $|I(\alpha_{max}) - I(\alpha_{min})| > \epsilon$, then $i = i + 1$ and replace $(\alpha_{min}, I(\alpha_{min})$ with $(\alpha_{max}, I(\alpha_{max})$ and go to step 4.
Stop: Stop the algorithm with $(\alpha_{max}, I(\alpha_{max}))$ as the optimal solution.

In the next section, this algorithm is evaluated with a test case.

8 Numerical Simulation

For these initial solutions, the right-angle profile ($\alpha = 0$), triangular profile ($\alpha = 1.2$), and circular profile ($\alpha = 1.0$) were selected. Figure 10 shows the Nusselt number distribution of these initial profiles.

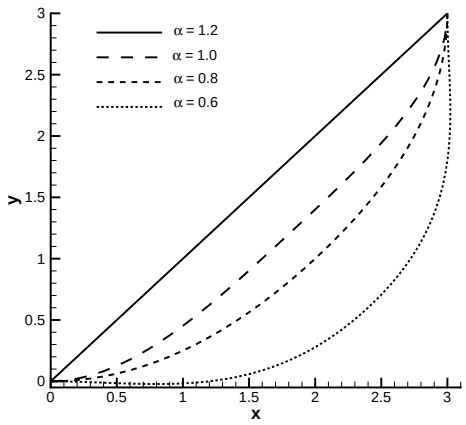

Figure 9: Some feasible curves.

The performance indices of these initial points are as follows:

$$I(0) = 1862.3,\ I(1.0) = 2470.1,\ I(1.2) = 2292.3$$

The second-degree polynomial that passed through these points was obtained by interpolation, as shown in Figure 10. The maximum of this polynomial occurred at $\alpha = 0.744$ with $I(0.744) = 2504$. The optimal solution was obtained at $\alpha = 0.751$, with $I(0.751) = 2510$ after ten iterations. The optimal profile and its related Nusselt number distribution are depicted in Figures 12 and 13, respectively. The result has 34% better performance with respect to the right-angle case, 1.62% better than the circular profile and 9.5% better than the triangular profile. This improvement was achieved for a single pin fin; therefore, when they are clustered to construct a heat sink, the overall performance will greatly increase. This improvement in heat transfer

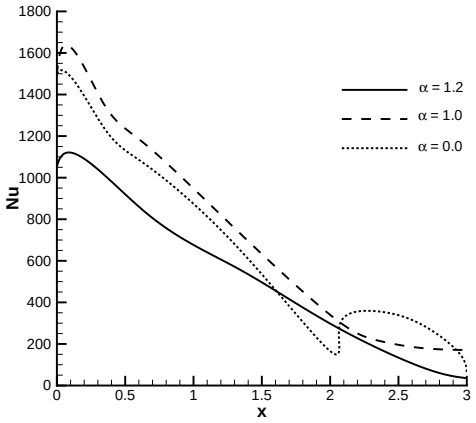

Figure 10: Nusselt number distribution for the chosen initial geometries.

specification of heat sinks will consequently decrease the power consumption of the cooling fans and result in electrical power savings.

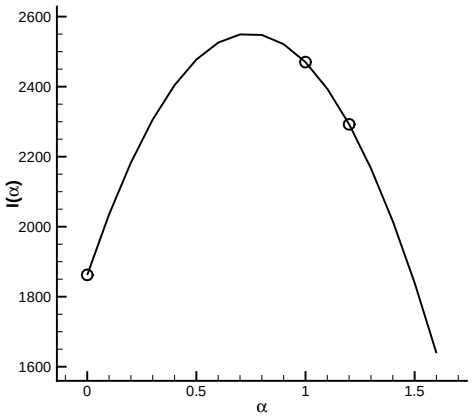

Figure 11: Interpolation curve for the initial solutions.

9 Conclusions

The problem of the optimal design of the connecting profile of a thermal pin fin was studied. Using parameterization with a cubic polynomial, the problem was formulated as a one-dimensional optimization problem. Then, a method based on interpolation was proposed to find the nearly

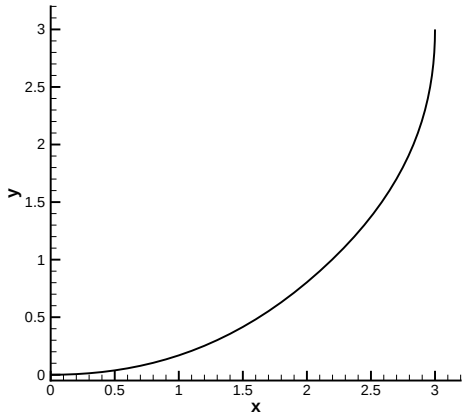

Figure 12: The resulting optimum curve.

optimal shape. These results may be used in the manufacturing of electrical devices in order to save energy and prevent depreciation.

For further research, other effective parameters such as the fin aspect ratio and the arrangement of fins in the heat sink plate could be considered.

Nomenclature

a, b, c, d, e, h: Geometrical parameters
A, B, C, D: Polynomial coefficients of C_1
A', B', C', D': Polynomial coefficients of C_2
A', B', C', D': Polynomial coefficients of C_2
F_1: Switch function in $(k - \epsilon)$ model
I: Performance index in the optimization problem
k: Turbulent Kinetic energy ($\mathrm{kgm^2s^2}$)
Pr: Prandtl number
Re: Reynolds number
$\overline{T}$: Average temperature (K)
U_i: Instantaneous velocity components ($\mathrm{ms^1}$)
$\overline{U_i}$: Mean velocity components ($\mathrm{ms^1}$)
u_i: Fluctuation velocity components ($\mathrm{ms^1}$)
$\overline{u_i u_j}$: Reynolds stresses ($\mathrm{m^2s^1}$)
α: Geometric parameter indicating admissible shapes
β, β^*, γ: Empirical constants in the SST model
μ: Viscosity ($\mathrm{kgm^1s^1}$)
μ_t: Eddy kinematic viscosity ($\mathrm{m^2\ s^1}$)

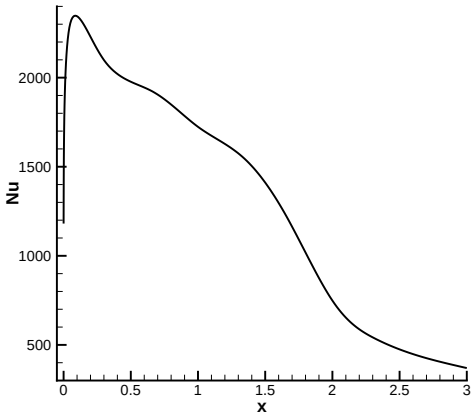

Figure 13: The Nusselt number distribution for the optimum curve.

ρ: Density (kg m^3)
$\sigma, \sigma_\omega, \sigma_{\omega 2}$: Empirical constants in the SST model
τ_{ij}: Reynolds stress tensor (kg m^1 s^2)
ω: Specific dissipation rate (s^1)

References

[1] Hamadneh N., Khan W. A., Sathasivam S., Ong H. C. (2013). "Design Optimization of Pin Fin Geometry Using Particle Swarm Optimization Algorithm", Plos One, 8, 1-9.

[2] Dede E. M., Joshi S. N., Zhou F. (2015). "Topology Optimization", Journal of Mechanical Design, 137, 111403 (2015).

[3] Klass Haertel J. H., Engelbrecht K., Lazarov B. S., Sig-mund O. (2015). "Topology Optimization of Thermal Heat Sinks", Proc. of COMSOL conference 2015, Grenoble, France, 1–6.

[4] Kayhani M. H., Norouzi M., Delouei A. A. (2012). "Analytical investigation of orthotropic unsteady heat transfer in compo-site pin fins", Modares Mechanical Engineering, 11, 21–32 (in Persian).

[5] Khan W. A., Culham J. R., Yovanovich M. M. (2005). "Optimization of Pin-Fin Heat Sinks Using Entropy Generation Minimization", IEEE Transactions on Components and Packaging Technologies, 28, 247-254.

[6] Shaukatullah H., Storr W. R., Hansen B. J., Gaynes M. A. (1996). "Design and Optimization of Pin Fin Heat Sinks for Low Velocity Applications", SEMI-THERM XII. Proceedings. Twelfth Annual IEEE.

[7] Pakrouh R., Hosseini M.J., Ranjbar A.A., Bahrampoury R. (2015). "A numerical method for PCM-based pin fin heat sinks optimization", Energy Conversion and Management, 103, 542-552.

[8] Mohammadian S. K., Zhang Y. (2015). "Thermal management optimization of an air-cooled Li-ion battery module using pin-fin heat sinks for hybrid electric vehicles", Journal of Power Sources, 273, 431-439.

[9] Park S. J., Jang D., Yook S. J., Lee K. S. (2015). "Optimization of a staggered pin-fin for a radial heat sink under free convection", International Journal of Heat and Mass Transfer, 87, 184-188.

[10] Bhanja D., Kundu B., Mandal P. K. (2013). "Thermal analysis of porous pin fin used for electronic cooling", Procedia Engineering, 64, 956–965.

[11] Javadi A., Javadi K., Taeibi-Rahni M., Keimasi M. (2002). "Reynolds Stress Turbulence Models for Prediction of Shear Stress Terms in Cross Flow Film Cooling–Numerical Simulation", ASME Pressure Vessels and Piping Conference, Vancouver, Canada.

[12] Herwig H. (2016). "What Exactly is the Nusselt Number in Convective Heat Transfer Problems and are There Alternatives?", Entropy, 18, 1-15.

[13] Corm A. R., Scheinberg K., Toint Ph. L. (1997). "Recent progress in unconstrained nonlinear optimization without derivatives", Mathematical Programming, 79, 397-414.

[14] Corm A. R., Scheinberg K., Toint Ph. L. (1997). "On the convergence of derivative-free methods for unconstrained optimization", in: A.Iserles, M. Buhmann (Eds.), Approximation Theory and Optimization: Tributes to M.J.D. Powell, Cambridge University Press, Cambridge, UK.

[15] Corm A. R., Scheinberg K., Vicente L. N. (2008). "Geometry of interpolation sets in derivative free optimization", Mathematical Programming, 111, 141-172.

[16] Patankar S. V. (1980). "Numerical heat transfer and fluid flow", McGraw-Hill, New York.

طراحی شکل بهینه برای پروفیل اتصال در یک پره خنک‌کننده

هاشمی مهنه، س. ح.
استادیار پژوهشگاه هوافضا-نویسنده مسئول
ایران، تهران، پژوهشگاه هوافضا
hmehne@ari.ac.ir

جوادی، خ.
استادیار گروه مهندسی هوافضا
ایران، تهران، دانشگاه صنعتی شریف، دانشکده مهندسی هوافضا، صندوق پستی ۱۱۳۶۵-۱۱۱۵۵
kjavadi@sharif.edu

تاریخ دریافت: ۲۶ آبان ۱۳۹۶ تاریخ پذیرش: ۹ اردیبهشت ۱۳۹۸

چکیده

در این مقاله یک مساله طراحی شکل بهینه در رابطه با بهینه‌سازی فین‌های خنک‌کننده قطعات رایانه‌ای و مدارهای مجتمع، مدل‌سازی و سپس حل می‌شود. هدف اصلی تعیین شکل یک فین دوبعدی است که به بیشترین برداشت حرارتی منجر شود. برای این منظور، مساله طراحی شکل بهینه بر اساس بیشینه‌سازی توزیع عدد ناسلت تعریف می‌شود. معادلات دیفرانسیل حاکم بر مساله در فازهای سیال و جامد به طور مستقل و همزمان حل می‌شوند. به منظور مدل‌سازی مساله بهینه‌سازی با بعد متناهی، شکل پروفیل به کمک منحنی‌های درجه سه پارامتری می‌شود. از آنجایی که رابطه صریحی بین تابع هدف مساله بهینه‌سازی با پارامتر هندسی وجود ندارد، از روش مدل‌سازی تقریبی در فرآیند بهینه‌سازی استفاده شده است. روش پیشنهادی با سه نقطه اولیه شروع می‌شود. سپس معادلات دیفرانسیل حاکم بر مساله برای هر یک از پروفیل‌های متناظر با این نقاط حل می‌شود. گام بعدی این روش تکراری شامل محاسباتی بر پایه درونیابی چندجمله‌ای بر روی مقادیر نرم اعداد ناسلت است. یک مثال عددی برای نشان دادن دقت و نحوه‌ی پیاده‌سازی روش ارائه شده است.

کلمات کلیدی

انتقال حرارت، بهینه‌سازی، بهینه‌سازی شکل، تقریب.